7-24-2017

Field Cracking Performance of Rigid Pavements

Yusuf Mehta
Rowan University, mehta@rowan.edu

Douglas Cleary
Rowan University

Ayman Ali

Recommended Citation

Mehta, Y., Cleary, D., & Ali, A. (2017). Field Cracking Performance of Rigid Pavements, Journal of Traffic and Transportation Engineering 4(4), 380-387.

JOURNAL OF TRAFFIC AND TRANSPORTATION ENGINEERING (ENGLISH EDITION) 2017; 4 (4): 380–387

Available online at www.sciencedirect.com

ScienceDirect

journal homepage: www.elsevier.com/locate/jtte

Original Research Paper

Field cracking performance of airfield rigid pavements

Yusuf Mehta [a,b,*], Douglas Cleary [a], Ayman W. Ali [b]

[a] Department of Civil and Environmental Engineering, Rowan University, Glassboro, NJ 08028, USA
[b] Center for Research and Education in Advanced, Transportation Engineering Systems (CREATEs), Rowan University, Glassboro, NJ 08028, USA

HIGHLIGHTS

- Reinforced isolation joints were not as effective in reducing the edge stresses as compared to thickened joints.
- Longitudinal cracking was more prevalent over asphalt base than over econocrete base for all three test sections.
- Slabs over the econocrete had greater percentage of corner cracks than the slab over the bituminous base.

ARTICLE INFO

Article history:
Received 16 November 2016
Received in revised form
30 April 2017
Accepted 4 May 2017
Available online 24 July 2017

Keywords:
Base layer
Corner cracking
Longitudinal cracking
Airfield rigid pavement

ABSTRACT

This paper discusses cracking in airport pavements as studied in Construction Cycle 6 of testing carried out at the National Airport Pavement Testing Facility by the Federal Aviation Administration. Pavements of three different flexural strengths as well as two different subgrades, a soft bituminous layer and a more rigid layer known as econocrete, were tested. In addition to this, cracking near two types of isolated transition joints, a reinforced edge joint and a thickened edge joint, was considered. The pavement sections were tested using a moving load simulating that of an aircraft. It has been determined that the degree of cracking was reduced as the flexural strength of the pavement was increased and that fewer cracks formed over the econocrete base than over the bituminous base. In addition, the thickened edge transition joint was more effective in preventing cracking at the edges compared to the reinforced edge joint.

1. Introduction

Cracking in concrete airport pavements is primarily caused by slow-moving heavy aircraft loading. Several factors are associated with the cracking or deterioration of the concrete pavements such as environmental conditions, joint performance, and subgrade material. To better understand the failure mechanism, full scale testing is conducted at the National Airport Pavement Testing Facility (NAPTF) in Atlantic

* Corresponding author. Department of Civil and Environmental Engineering, Rowan University, Glassboro, NJ 08028, USA. Tel.: +1 856 256 5320; fax: +1 856 256 5242.
E-mail addresses: mehta@rowan.edu (Y. Mehta), cleary@rowan.edu (D. Cleary), alia@rowan.edu (A. W. Ali).
Peer review under responsibility of Periodical Offices of Chang'an University.
http://dx.doi.org/10.1016/j.jtte.2017.05.010

City, New Jersey in which all three factors were evaluated. One of the objectives of the testing of Construction Cycle 6 at this facility was to evaluate the influence of concrete flexural strength and two different support conditions on pavement performance. The long term performance of pavement is directly related to the stability of the subgrade material supporting the various layers in the pavement structure. Without suitable subgrade, the pavement will ultimately experience excessive bending thus causing premature cracking and deterioration throughout its lifespan. In addition to evaluating the subgrade material, two types of isolation joints were compared to assess which type of joint performed better overall in preventing deterioration of the concrete slabs in each MRS section. The authors have already presented the load transfer efficiency of these doweled and isolation joints under full scale testing (Cunliffe, 2013). This paper was formulated to present the results of the full scale testing performed on the pavement. It should be noted, however, that a detailed evaluation of the performance of slabs and isolation joints is not presented.

2. Objectives

The objectives of this study were as follows.

1) To quantify the deterioration and formation of cracking in three different flexural strength concrete pavements under dynamic loading.
2) To determine the influence of the stiffness of the stabilized base layer on the cracking patterns.
3) To evaluate the performance of two different types of isolation joints.

3. Significance of study

The results of this study provided useful insight into the influence of rigid pavement flexural strength and the influence of base layer stiffness on cracking behavior under full scale testing. The type of cracking that forms and quantification of cracks provides insight into how the stiffness of the base layer, the flexural strength of the pavement, and the type of joint used in connect slabs affects cracking behavior. This cracking pattern would provide an understanding into how isolation transition joints and support conditions respond to long term repeated loading.

4. Test sections characteristics

Full scale testing at the National Airport Pavement Testing Facility has been conducted to evaluate pavement performance as well as dowel joint performance and isolation transition joint performance over different stabilized base layer types and with different flexural strength concretes. The test pavement, shown in Fig. 1, consists of 10-inch concrete pavements of three different target flexural strengths. MRS-1 corresponds to a low flexural strength pavement (28-day strength of 500 psi), and MRS-3 corresponds to a high flexural strength (28-day strength of 1000 psi) pavement. Each of these flexural strength pavements is divided into north and south test sections, where the north test section has a 6-inch bituminous stabilized base layer beneath the concrete pavement and the south test section has a 6-inch econocrete stabilized base layer beneath the concrete pavement. As depicted, there are two additional layers

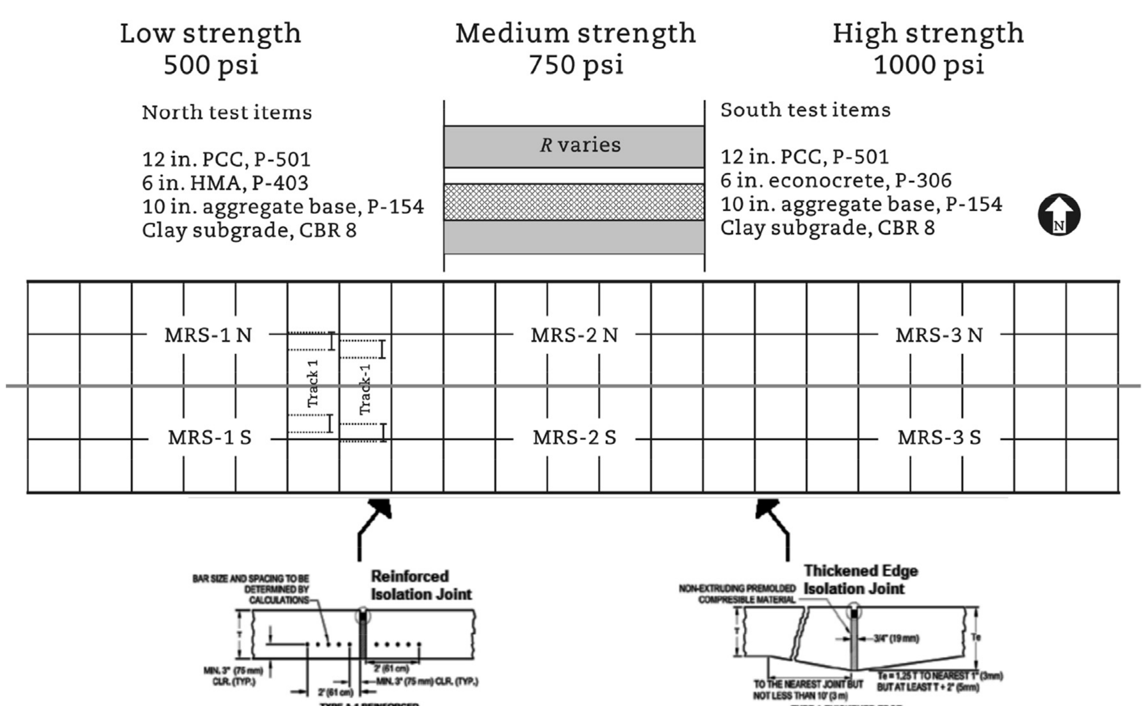

Fig. 1 – Test pavement composed of different flexural strength pavements on different stabilized base layers and the positions of different joint types (Cunliffe, 2013).

beneath the stabilized base; a 10-inch crushed aggregate subbase layer and a clay subgrade layer which can be assumed to be infinite in depth. It should be noted however, that the average achieved target 28-day flexural strengths for sections MRS-1, MRS-2, and MRS-3 were 661, 566, and 643 psi, respectively.

Dynamic loading was applied by a loading carriage that simulated aircraft loading over the test pavement which consisted of a two wheel pattern. The load was applied along nine different tracks to simulate aircraft wander patterns, for example: track 0, 1, −1, 2, −2,⋯, where each of the non-zero tracks corresponds to an offset distance measured with reference to track 0. This offset distance was set to be equal on both sides of track 0. The loading magnitude, shown in Table 1, was increased in steps to the completion of dynamic loading, to intensify and hasten the cracking and deterioration process in the pavement. The cracking process was accelerated to provide results of the lifetime performance of the airport pavement without the full time period required to achieve the same results.

Table 1 contains the number of passes that each MRS section experienced as well as the loading that was applied during each pass. A preloading of 44 kips was conducted on MRS-1 on the north track only to provide an estimate on how the pavement would react to the full scale testing. The preloading was then followed by the first set of initial passes which consisted of each of the MRS sections experiencing the same 15,708 passes at a wheel loading of 45 kips per wheel. After the first set of passes was completed, the second set of passes was conducted in which only MRS-2 and MRS-3 sections were tested with a wheel loading of 52 kips per wheel. MRS-1 was not loaded further (i.e., at the 52 kips loading range) due to excessive deterioration and cracking as determined by the NAPTF after applying the 45 kips loading range. After the second testing cycle the MRS-3 section was determined to withstand the testing so the wheel loading was increased to 70 kips per wheel to induce cracking during the third cycle of testing. During the testing of the third set of passes only MRS-2 and MRS-3 sections were tested with a 52 kip per wheel loading applied to MRS-2 and a 70 kip per wheel loading applied to MRS-3.

Between each of the slabs for a given MRS section are both transverse and longitudinal dowel joints connecting adjacent slabs. These joints are designed with the intention of reducing slab stresses, strains and deflections in a slab edge by transferring the load from the loaded slab to the adjoined unloaded slab. The load transfer across joints is meant to extend the lifetime of a concrete pavement by reducing cracking and deterioration in the slab edges. The two isolation transition joint types, depicted in Fig. 1, were used in Construction Cycle 6 (CC6) and can be found between adjacent MRS sections. The two isolation transition joints types, the reinforced edge and thickened edge joints, are designed to sustain or reduce slab edge stresses without transferring any loading from a loaded slab to an adjacent unloaded slab. This is done by strengthening the edge either through steel reinforcement along the edge of the slab (reinforced edge joint) or by increasing the depth of the concrete at the edges of the slab and introducing an isolation form between the slabs which would therefore prevent load transfer through interlock.

Table 1 – Dynamic loading for different pass sets.

Date	Pass set	Wheel load (lbs.)	Pass		
			MRS-1	MRS-2	MRS-3
7/8/11–8/15/11	Preloading[a]	44,000	6790	0	0
8/30/11–12/20/11	463–15,708	45,000	15,708	15,708	15,708
12/27/11–2/29/12	15,709–26,729	52,000	0	11,022	11,022
3/1/12–4/25/12	26,730–39,203	52,000	0	12,473	0
		70,000	0	0	12,473
		Total passes	22,498	39,203	39,203

Note:
[a] Loading had been conducted on MRS-1 north prior to the conduction of full scale testing.

5. Results

Each MRS section was examined daily for cracks and overall deterioration, once in the morning and once in the evening after the passes had been completed. The "crack map" was created for each MRS section to show the type of crack and the date the crack appeared on the slab. The "crack map" for one of the MRS section is shown in Fig. 2. The cracks were numbered based on the date the crack formulated, but under close evaluation saw cuts (shown as cross marks or circles on the maps) that had been made to examine the deflection gauges inside the slabs were counted as cracks. These cracks, number 15–44, were ignored during the analysis of the pavements cracking behavior. It is important to note that no additional cracks or gaps had propagated from these saw cuts which would unfairly influence the data results. The quantification of the results is tabulated in Tables 2 and 3 which contain the same data, but are presented in two important iterations. Table 2 consists of the total quantification of the cracks with respect to the flexural strength and highlights the difference in north and south slabs. Table 3 contains the total number of cracks formed while highlighting the number of passes to the formation of the cracking.

5.1. *Cracking in MRS-1*

In MRS-1, the dynamic loading had been conducted on the bituminous base section prior to testing on all other sections, which contributed to the earlier deterioration of the slab in comparison to the higher flexural strength sections. The north section of MRS-1 was tested initially after all slabs were formed to induce early age cracking in the slabs. The preloading period started in August of 2011 and lasted until the first day of September when the first set of passes began. Saw cuts were made on August 25, 2011 to check deflection gauges which were labeled as cracks in Fig. 2, but were not included in the analysis of total cracking examined on each MRS section. Fig. 2 details the complete cracking over the course of testing, where each color corresponds to a set of numbered cracks on a specified date. As shown, the vast majority of early cracks formed on the bituminous base concrete slab section in sections were connected by dowel joint. Cracking continued

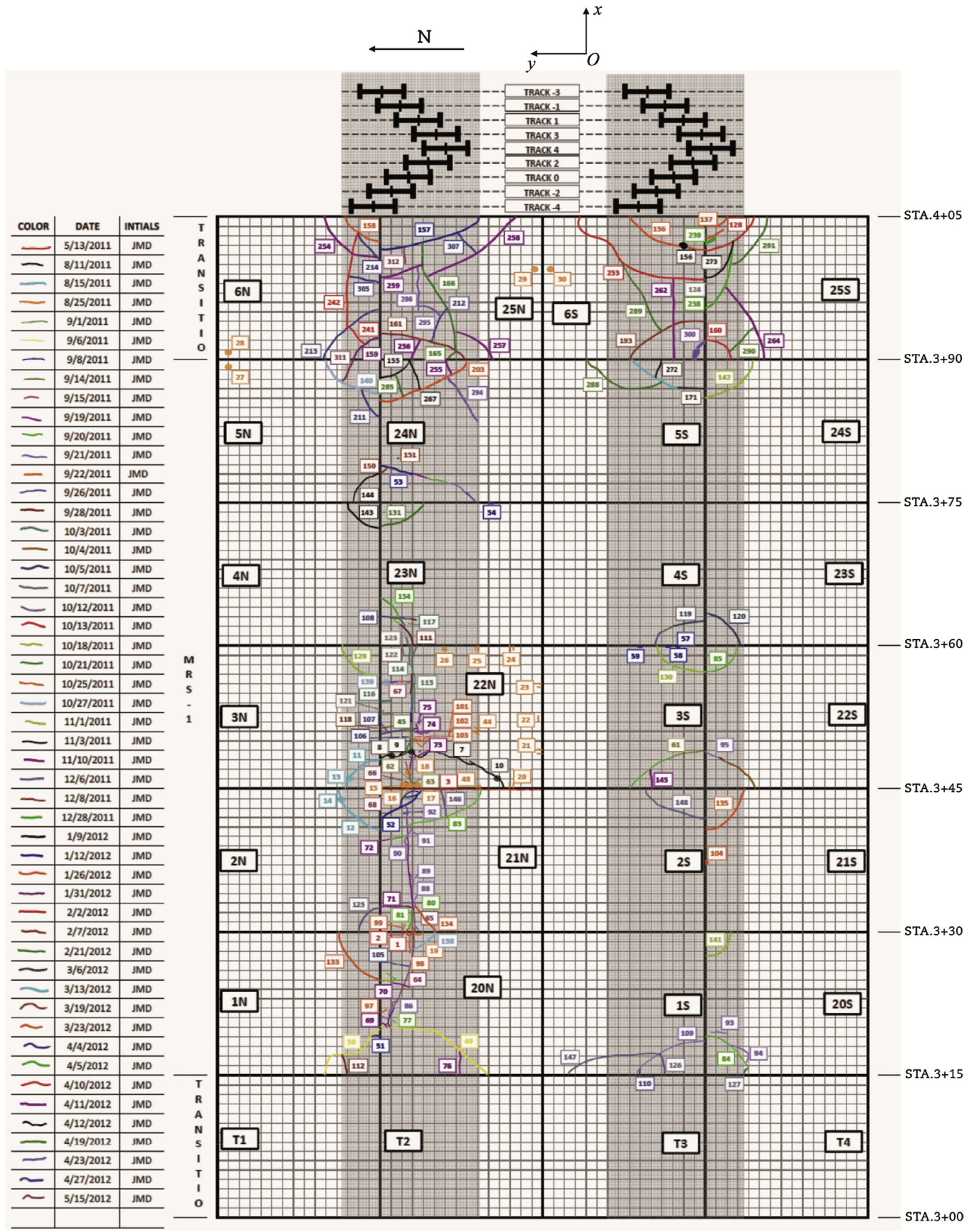

Fig. 2 – Cracking detail for medium-strength subgrade rigid pavement section 3 placed on a stabilized base, MRS-1 (Federal Aviation Administration, 2012).

on both stabilized base layers during the course of testing for slabs were connected by dowel joints. It isn't until later passes, after MRS-1 had been declared sufficiently deteriorated, that cracks began to form along the slab edges at the isolation transition joint, specifically at the reinforced joint for this section. The quantity of cracks formed on the north section of the track near the reinforced isolation joints was noticeably greater, as well as on the entire north section of the track for MRS-1 compared to the south section. The joint between slabs 23N and 24N on the north section and 4S and 5S on the south section is important to be noted. Corner cracks developed on the north side of the track while no

Table 2 – Quantification of total cracking based on flexural strength.

Section	Target flexural strength (psi)	Base layer	Number of cracks	Total crack
MRS-1	500	North (bituminous base)	113	155
		South (econocrete base)	42	
MRS-2	750	North (bituminous base)	46	68
		South (econocrete base)	22	
MRS-3	1000	North (bituminous base)	33	54
		South (econocrete base)	21	

Table 3 – Quantification of total cracking based on number of passes.

Number of passes	MRS-1		MRS-2		MRS-3	
	North	South	North	South	North	South
Preloading	11	0	1	0	2	0
0–15,708	73	26	2	2	1	0
15,709–26,729	7	2	2	1	0	0
26,730–39,203	22	14	41	19	30	21

cracks developed at the joint on the south side at the same loading conditions and number of passes while showing different signs of distress. The exact quantification of these results is tabulated in Tables 2 and 3

5.2. *Cracking in MRS-2*

The detailed cracking pattern throughout testing for MRS-2 (figure was not shown in the interest of brevity), showed that few cracks form over the initial set of dynamic passes. Many of the cracks forming over the pavement appeared mid-way through the completion of testing, with both longitudinal and corner cracks forming in slabs connected with dowel joints. Around the same time as these cracks are forming, cracks are also forming at the reinforced isolation transition joint edge adjacent to the MRS-1 section. Cracking on the thickened edge isolation transition joint slabs does not occur until late into the full course of testing for the bituminous base section and not at all on the econocrete base section. It should also be noted that there were considerably fewer cracks formed on concrete slabs in MRS-2 as compared to MRS-1 even though MRS-2 was loaded with higher loads throughout testing. Longitudinal cracks were more significant on the north section of MRS-2 compared to the south section which had only one longitudinal crack and considerably more corner cracks. The slabs on the north section of MRS-2 near the thickened edge isolation joint showed more signs of distress compared to the south section. Longitudinal and corner cracks were noticeable on the north section while no cracks formed on the south section. It is also important to note small deformations were noted on a section of the track between slabs 31N and 32N.

5.3. *Cracking in MRS-3*

The same loading was applied to both the north and south sections and the slabs were not pre-loaded before testing. Initial testing consisted of a 45 kip load passing over MRS-3 a total 15,708 times and produced only a few initial cracks. The cracking pattern throughout testing for MRS-3 showed that they were formed on both the north and south during the midway point of testing. Longitudinal cracks were more noticeable on the north section, while corner cracks and “potholes” were noted on the south section. Compared to the other sections, MRS-3 had the fewest cracks, but had more “potholes” forming on the south section. The slabs which were connected by reinforced edge joints showed minimal cracking which was developed midway during loading. Three cracks formed on these slabs which included two longitudinal cracks and a transverse crack. The slabs on the south test section which were connected with the reinforced edge joints had no crack form during the entire testing period.

6. Discussion

6.1. *Performance of slabs adjacent to dowel joints (evaluation of flexural strength and base layer)*

The target flexural strengths of the three sections, MRS-1, MRS-2, and MRS-3, were 500, 750, and 1000 psi, respectively. The extent of cracking in MRS-1 was significantly greater than that in MRS-3 which had heavier loads and more load passes. The higher flexural strength of the pavements was attributed to the resistance of the concrete pavement to cracking since the reduction in cracks was not segregated to either the north or south section of the pavement, but on the entire MRS section. The flexural strength of concrete determined what type of crack was formed on the pavement surface. The increase in flexural strength of the concrete reduced the stress on the pavement and prevents corner and longitudinal cracks from forming (Zoorob et al., 2002). Changing the thickness of the slab also determined what type of crack was formed on the pavement surface. Stress was reduced in the slab when the slab thickness was increased. When the stresses were reduced, corner cracking and longitudinal cracking were prevented. The load transfer efficiency of the joint would help reduce stresses in a slab that is dowel jointed, but would only help to prevent corner cracking because the stress being reduced from the load transfer was only affecting the joints and edges. Table 2 shows a quantitative relationship between the flexural strength and the number of cracks formed.

The north testing section, consisting of a 6-inch bituminous base was noted as having significantly more cracks formed as compared to the south testing section, consisting of a 6-inch econocrete subgrade. The north test section had a total of 192 cracks compared to the south test section, where only 85 cracks formed. More specifically, for each MRS section the comparisons in Tables 2 and 3 show that for each section, more cracking occurred on the north side. The increase in cracks in the north side was due to the higher stresses in the PCC slab constructed over a flexible bituminous base. On the other hand, the slab constructed over the cement stabilized base had better support and hence tensile stresses were lower in the slab causing fewer cracks. The schematic of the difference in stress distribution over the two bases is shown in

Fig. 3. The south testing section which consisted of a 6-inch bituminous base was not pre-loaded in this study to induce early age cracking.

Full scale testing on the MRS sections was completed on April 25, 2012 in which the PCC slabs experienced a total of 39,203 passes. Fig. 3 shows the quantity of cracks is related to the number of passes. It is important to emphasize that the north testing section of MRS-1 was preloaded with a 44 kip dynamic loading. The first set of passes, consisting of passes 0–15,708, had a dynamic wheel loading of 45 kips for all MRS sections. The second set of passes consisted of passes 15,709–26,729 with a dynamic wheel loading of 52 kips for MRS-2 and MRS-3 only since MRS-1 had deteriorated beyond the point of further testing. The third set of passes consisted of passes 26,730–39,203 with a dynamic wheel loading of 52 kips for MRS-2 and 70 kips for MRS-3. The loads were varied between MRS-2 and MRS-3 because the flexural strength of MRS-3 had proved to be more resilient to cracking than previously thought for the 52 kip load so a more significant dynamic load was applied to MRS-3 to induce cracking.

Fig. 3 illustrates that MRS-1 had the largest amount of cracks, especially in the earliest stage of the full scale testing. MRS-1 experienced the most cracking during the first set of passes of full scale testing in which 98 cracks were developed. MRS-2 and MRS-3 experienced the most cracking in the final stage of full scale testing. MRS-3 had the least amount of cracking even though it had the largest dynamic loading of 72 kips applied to the slabs which showed the resilience of the flexural strength of the PCC.

Cracks were still forming on MRS sections even when that specific section was not receiving dynamic load potentially. This is because of heavy weight deflectometer testing and the fact that it is connected to the MRS section which is experiencing the loading stresses.

6.2. *Longitudinal crack*

Comparing the north and south sections of all the MRS sections shows that longitudinal cracks were more common on the north section. This could be accounted for in the bituminous base that was used for the north section which is a softer base layer. The tensile stresses caused by the tires moving on the pavement could have caused the longitudinal cracks which go parallel to the movement of the tires. The south section had an econocrete base which is a more rigid base layer. The cracks that formed on this section of the pavement were corner cracks caused by fatigue damage accumulation on the pavement. The tensile stresses of the tire did not affect the pavement as much as in the north section of the pavement since longitudinal cracks were not common in the south sections of all MRS sections. Table 4 shows the amount of longitudinal cracks formed on the concrete slabs for all north and south sections of all MRS sections. The loading of 44 kips was conducted on the north side of MRS-1 to induce longitudinal cracking during the preloading period before full scale testing was started. Full scale testing started on September 1, 2011 after the north section of MRS-1 had already experienced 6790 passes.

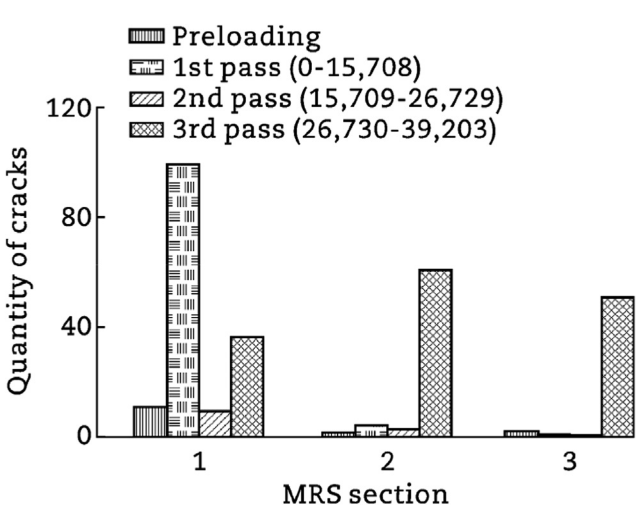

Fig. 3 – Quantity of cracks versus number of loading passes.

6.3. *Corner crack*

Comparing the north and south testing sections of each MRS section shows that corner crack was more prevalent in the south testing section which consisted of a 6-inch econocrete base layer. The highest percentage of corner cracking occurred in the south testing section in MRS-2 with 91% of corner cracks. Each MRS section had a higher percentage of corner cracks in the south testing section with MRS-1 having 55% of corner cracks, MRS-2 having 91% of corner cracks, and MRS-3 having 86% of corner cracks. Table 5 contains the quantification of corner cracks for each MRS section and in the north and south testing sections.

The corner cracks which formed on each MRS section were caused by fatigue damage due to stresses caused by the number of passes and load increments of each pass. Previous pavements, such as Construction Cycle 2 (CC2) which was tested at the NAPTF, had a majority of longitudinal cracks under dynamic loading (Brill et al., 2009). Test pavement CC2 consisted of three different sections which were designated based on subbases: medium rigid conventional base (MRC), medium rigid directly on grade (MRG), and medium rigid stabilized base (MRS). Transverse and corner cracks were rare in all three types of subbases used in CC2. The only comparison that can be made between the two testing Construction Cycles is between the MRS section of CC2 and all three MRS sections of CC6. The PCC in the MRS slab in CC2 had an average field flexural strength of 655 psi with a 6-inch econocrete base layer. A dynamic load of 55 kips was held constantly throughout testing in CC2 with a 6-wheel configuration used on the north testing section while a dual tandem wheel configuration was used on the south testing section. The wheel configuration was altered between testing sections to determine how the application of the loading was distributed among the wheels. It is important to note that the cracks that formed on CC2 were longitudinal instead of corner cracks, which shows a discontinuity between results. This discontinuity can potentially be explained by the differences in flexural strength of the PCC or the wheel configuration in which CC2 had a six-wheel

Table 4 – Number of longitudinal cracks.

Section	Target flexural strength (psi)	Base layer	Longitudinal cracks	Total cracks
MRS-1	500	North (bituminous base)	25	26
		South (econocrete base)	1	
MRS-2	750	North (bituminous base)	7	8
		South (econocrete base)	1	
MRS-3	1000	North (bituminous base)	9	9
		South (econocrete base)	0	

Table 5 – Number of corner cracks.

Section	Base layer	Number of corner cracks	Total number of cracks	Percentage of corner cracks (%)
MRS-1 (500 psi)	North (bituminous base)	33	113	29
	South (econocrete base)	23	42	55
MRS-2 (750 psi)	North (bituminous base)	26	46	57
	South (econocrete base)	20	22	91
MRS-3 (1000 psi)	North (bituminous base)	10	33	30
	South (econocrete base)	18	21	86

Table 6 – Quantification of cracks with different isolation transition joints.

Isolation transition joint type	Target flexural strength (psi)	Base layer	Number of cracks	Total cracks
Reinforced	500–750	North (bituminous base)	34	56
		South (econoncrete base)	22	
Thickened edge	750–1000	North (bituminous base)	9	9
		South (econoncrete base)	0	

vehicle configuration on the north testing section applying the load instead of a dual tandem wheel configuration that was used for all testing sections in CC6 (Cunliffe, 2013).

6.4. *Performance of slabs adjacent to isolation transition joints*

The joints which connected MRS-1 to MRS-2 and MRS-2 to MRS-3 were varied to determine how different isolation joints would respond to dynamic loading. Both sets of slabs had 39,203 total passes throughout the testing with the only difference occurring during the last set of passes (26,730–39,703) in which the thickened edge joints experienced a heavier 70 kip dynamic load while the reinforced isolation joints had only 52 kip dynamic load. The joints connecting MRS-1 to MRS-2 consisted of reinforced isolation joints which had significantly more degradation and cracking compared to the joints connecting MRS-2 to MRS-3, which had consisted of thickened edge isolation joints. The slabs which were connected via reinforced isolation joints had more signs of distress, where 56 cracks formed on the slabs compared to the slabs connected via thickened edge joints. The thickened edge isolation joint slabs had only 9 cracks form throughout testing. The cracks which did form on the thickened edge isolation joint slabs consisted of longitudinal cracking whereas the cracks which formed on the reinforced isolation joints were corner and transverse cracks. Table 6 contains the quantification of cracks that formed on the slabs which were connected via isolation transition joints.

The rest of the slabs on the MRS sections were connected through dowel joints which were supposed to distribute the stresses caused by the dynamic loading to the adjacent slabs. The thickened edge joints had less cracks on the slabs as compared to the dowel jointed slabs for all MRS sections which appeared to indicate that the dowel jointed slabs were not transferring the load effectively. Isolation transition joints are designed with the purpose of reducing stresses in the edges of pavement and allow pavement expansion. Fares (2009) showed that the isolated transition, specifically thickened edge transition, was best used to reduce and control cracking or damage in the slab. This study supports this conclusion since the slabs which were connected via thickened edge transition joints experienced the least amount of cracks although it is noted that a thickened edge joint is more difficult to construct.

7. Conclusions

The conclusions based on the study are as follows.

(1) In each MRS section, the slabs (north side) over a 6-inch bituminous contained more cracks as compared to the slabs (south side) over a 6-inch econocrete base layer.
(2) The north side of the track also contained more longitudinal cracks compared to the south side. There were a total of 41 longitudinal cracks formed on the north side

of all the MRS sections as compared to only 2 on the south section.

(3) As the flexural strength of the PCC layer increased in MRS-1 (500 psi), MRS-2 (750 psi), and MRS-3 (1000 psi), the amount of cracks in each section decreased as 155, 68 and 54, respectively.
(4) The slabs with reinforced isolation joints experienced more cracking (56 cracks) as compared to the thickened isolation joints which had only 9 cracks.
(5) The percentage of corner cracks in PCC over econocrete was greater than that of PCC over bituminous base.
(6) Even though the number of cracks in MRS-2 and MRS-3 were about 60% less than MRS-1, the percentage of corner cracks in MRS-2 and MRS-3 over econocrete base was 91% and 86% respectively.
(7) Longitudinal cracking was more prevalent over asphalt base than over econocrete base for all three test sections.
(8) Thickened edge joints had least amount of cracks on the slabs compared to both the reinforced isolation joints and the dowel jointed slabs for all MRS sections which showed that the thickened edge joints kept the stresses lower at the edge of the slabs.
(9) Slabs over the econocrete had greater percentage of corner cracks than the slab over the bituminous base.
(10) The reinforced isolation joints were not as effective in reducing the edge stresses as compared to thickened joints
(11) Pavements with lower flexural strength PCC (MRS-1) had a higher number of cracks than higher flexural strength pavements.

Acknowledgments

The authors would like to acknowledge the Federal Aviation Administration (FAA) as this work is funded under FAA research grant #10-G-012. Although this project has been sponsored by the FAA, it should be known that the content of the paper reflect the views of the authors, who are responsible for the facts and accuracy of the data presented within. The content do not necessarily reflect the official views and policies of the FAA. This paper does not constitute a standard, specification, or regulation.

REFERENCES

Brill, D.R., Hayhoe, G.F., Ricalde, L., 2009. Analysis of CC2 Rigid Pavement Test Data from the FAA's National Airport Pavement Test Facility. Federal Aviation Administration, Washington DC.

Cunliffe, C., 2013. Joint Load Transfer of Construction Cycle 2 and Construction Cycle 6 Concrete Airfield Pavements at the National Airport Pavement Test Facility: Final Report. Rowan University, Glassboro.

Fares, A., 2009. Cement-Stabilized Base Courses. Portland Cement Association, Skokie.

Federal Aviation Administration (FAA), 2012. Concrete Construction Cycle 6 Crack Map Imagery. National Airport Pavement Test Facility, Atlantic City.

Zoorob, S.E., Collop, A.C., Broun, S.F., 2002. Performance of Bituminous and Hydraulic Materials in Pavements. CRC Press, Boca Raton.

Yusuf Mehta, PhD, P.E. is a professor and the director of Center for Research and Education in Advanced Transportation Engineering Systems. He has an outstanding research record in pavement materials. Dr. Mehta has extensive experience on several research projects with New Jersey, Florida, Wisconsin and Rhode Island Departments of Transportations, Federal Highway Administration and Federal Aviation Administration. Since coming to Rowan University, Dr. Mehta has received approximately $10 million dollars of external funding in pavements and materials.

Douglas Cleary, PhD, P.E. is an associate professor in the Department of Civil and Environmental Engineering. He has conducted pavement research for New Jersey Department of Transportation NJDOT and the Federal Aviation Administration including the use of recycled materials in concrete and evaluation of full scale pavement testing data from the FAA Technical Center. He also has research experience and interests in many aspects of reinforced concrete including reinforcing steel anchorage, external FRP reinforcement, airport pavements, and self-consolidating concrete. His current research includes investigation of structural steel connections including time-dependent loss of clamping force and connections employing fabric reinforced resin thermal barrier plates. He has managed technical workshops on seismic engineering. He has been awarded the New Jersey Section ASCE Educator of the Year. He has served as the associate chair of his department and is the affiliate director of Project Lead the Way in New Jersey.

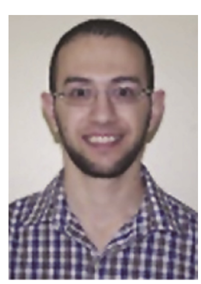

Ayman W. Ali, PhD, serves as the manager of the Center for Research and Education in Advanced Transportation Engineering Systems (CREATEs) at Rowan University. Dr. Ali has served as a collaborative principal investigator on multiple projects funded by the New Jersey Department of Transportation (NJDOT). He also served and successfully completed, as a leading researcher, projects funded by the Ohio Department of Transportation (ODOT), Rhode Island Department of Transportation (RIDOT), the Federal Highway Administration (FHWA), and the Federal Aviation Administration (FAA). The scope of his projects have covered a wide range of research topics including, but were not limited to, characterizing the performance of pavement materials or additives (both asphalt binder and mixtures), investigating new technologies for use as compaction quality control methods, developing specifications for using these new technologies, determining the life expectancy of various HMA overlay mixes, developing computer software tools for generating specific mechanistic empirical pavement design guideline inputs for the state of Ohio, determining the limitation of warm mix asphalt produced using foamed asphalt binders (WMA-FA), and characterizing the laboratory and field performance of WMA-FA mixtures.